Journal of Geochemical Exploration 165 (2016) 159–173

Contents lists available at ScienceDirect

Journal of Geochemical Exploration

journal homepage: www.elsevier.com/locate/gexplo

Indicator mineral-based exploration for carbonatites and related specialty metal deposits — A QEMSCAN® orientation survey, British Columbia, Canada

D.A.R. Mackay [a], G.J. Simandl [a,b,*], W. Ma [c], M. Redfearn [c], J. Gravel [d]

[a] School of Earth and Ocean Sciences, University of Victoria, 3800 Finnerty Rd., Victoria, British Columbia V8P 5C2, Canada
[b] British Columbia Geological Survey, Ministry of Energy and Mines, P.O. Box 9333, Stn Prov Govt., 5th floor-1810 Blanshard St., Victoria, British Columbia V8W 9N3, Canada
[c] Bureau Veritas Commodities Canada Ltd., Inspectorate Metallurgical Division, 11620 Horseshoe Way, Richmond, British Columbia V7A 4V5, Canada
[d] Bureau Veritas Commodities Canada Ltd., Upstream Minerals Sector, 9050 Shaughnessy St., Vancouver, British Columbia V6P 6E5, Canada

ARTICLE INFO

Article history:
Received 24 February 2015
Revised 18 January 2016
Accepted 6 March 2016
Available online 10 March 2016

Keywords:
Indicator mineral
QEMSCAN
Specialty metals
Carbonatite
Exploration
Orientation survey

ABSTRACT

This orientation survey indicates that Quantitative Evaluation of Materials by Scanning electron microscopy (QEMSCAN®) is a viable alternative to traditional indicator mineral exploration approaches which involve complex processing followed by visual indicator mineral hand-picking with a binocular microscope. Representative polished smear sections of the 125–250 μm fraction (dry sieved and otherwise unprocessed) and corresponding Mozley C800 table concentrates from the drainages of three carbonatites (Aley, Lonnie, and Wicheeda) in the British Columbia Alkaline Province of the Canadian Cordillera were studied. Polished smear sections (26 × 46 mm slide size) contained an average of 20,000 exposed particles. A single section can be analyzed in detail using the Particle Mineral Analysis routine in approximately 3.5–4.5 h. If only mineral identification and mineral concentrations are required, the Bulk Mineral Analysis routine reduces the analytical time to 30 min.

The most useful carbonatite indicator minerals are niobates (pyrochlore and columbite), REE-fluorocarbonates, monazite, and apatite. Niobate minerals were identified in the 125–250 μm fraction of stream sediment samples more than 11 km downstream from the Aley carbonatite (their source) without the need for pre-concentration. With minimal processing by Mozley C800, carbonatite indicator minerals were detected downstream of the Lonnie and Wicheeda carbonatites. The main advantages of QEMSCAN® over the traditional indicator mineral exploration techniques are its ability to: 1) analyze very small minerals, 2) quickly determine quantitative sediment composition and mineralogy by both weight percent and mineral count, 3) establish mineral size distribution within the analyzed size fraction, and 4) determine the proportions of monomineralic (liberated) grains to compound grains and statistically assess mineral associations in compound grains. One of the key advantages is that this method permits the use of indicator minerals based on their chemical properties. This is impossible to accomplish using visual identification.

1. Introduction

Canada has excellent potential for discovery of new specialty metal deposits (Simandl et al., 2013). Potential shortages in specialty metal supply has caused price spikes in the price of Ta_2O_5 and a steady increase in the price of ferroniobium (Mackay and Simandl, 2014a). This has fuelled interest in carbonatite-related deposits. To improve the effectiveness of Canadian companies, there is a need for development of new, or customization of existing, exploration methods. This study assesses the use of Quantitative Evaluation of Materials by Scanning electron microscopy (QEMSCAN®) for identification of carbonatite and related specialty metal deposit indicator minerals in stream sediments. This also determines if automated analysis allows for indicator mineral studies which forgo the need for heavy liquid separation, relying on dry sieving and gravity table separation.

Traditional indicator mineral exploration methods for gold, kimberlite, and metamorphosed or magmatic massive sulfide deposits are described by Averill (2001, 2014), McCurdy et al. (2006, 2009), and McClenaghan (2011, 2014). These studies utilize the 0.25–2.0 mm heavy mineral fraction of unconsolidated surficial sediments. Sediment samples are pre-concentrated (typically using a shaker table) before heavy liquid separation, isodynamic magnetic separation, and optical identification and hand-picking (McClenaghan, 2011). The concentrate is then sieved and the 0.5–1 mm and 1 to 2 mm fractions are visually examined, and indicator minerals are counted and hand-picked while the 0.25–0.5 mm fraction is subject to paramagnetic separation before

* Corresponding author at: British Columbia Geological Survey, Ministry of Energy and Mines, P.O. Box 9333, Stn Prov Govt., 5th floor-1810 Blanshard St., Victoria V8W9N3, Canada.
E-mail address: George.Simandl@gov.bc.ca (G.J. Simandl).

http://dx.doi.org/10.1016/j.gexplo.2016.03.005
0375-6742/

Table 1
Potential indicator minerals for carbonatite-related deposits, their density, and corresponding pathfinder elements. Typical grain sizes for indicator minerals from carbonatites and related deposits are shown (from Mäder, 1986; Brod, 1999; Belousova et al., 2002a,b; Anthony et al., 2004; Trofanenko, 2014; Chakhmouradian et al., 2015).
Modified from Mackay et al., 2015b.

Mineral name	Chemical formula	Density (g/cm^3)	Main pathfinder elements (s)	Average size (mm)
Pyrochlore	$(Ca,Na)_2(Nb,Ti,Ta)_2O_6(O,OH,F)$	4.2–6.4	Nb	0.01–4 μm; 2 cm*
Columbite-(Fe)	$(Fe,Mn)(Ta,Nb)_2O_6$	5.3–7.3	Nb	10 μm–1.5 mm
Fersmite	$(Ca,Ce,Na)(Nb,Ta,Ti)_2(O,OH,F)_6$	4.69–4.79	Nb	<10–200 μm
Monazite	$(Ce,La,Nd,Th)PO_4$	4.8–5.5	LREE, Th, P	10–50 μm
Zircon	$ZrSiO_4$	4.6–4.7	Zr, U	10 μm–5 mm
Bastnaesite	$Ce(CO_3)F$	4.95–5.00	LREE	4 μm–1 mm
Synchysite	$Ca(Ce,La)(CO_3)_2F$	3.90–4.15	LREE	<2 μm–1 mm; 6 cm*
Apatite	$Ca_5(PO_4)_3(OH,F,Cl)$	3.16–3.22	P	0.05–0.5 cm; >1 cm*
Barite	$BaSO_4$	4.48	Ba	10–50 μm, 1–5 mm*
Celestine	$SrSO_4$	3.9–4.0	Sr	
Magnetite	Fe_3O_4	5.1–5.2	Fe	1–2 cm
Arfvedsonite	$Na_3[(Fe,Mg)_4Fe]Si_8O_{22}(OH)_2$	3.44–3.45	n.a.	<0.5 mm
Richterite	$Na(Ca,Na)(Mg,Fe)_5(Si_8O_{22})(OH)_2$	3.09	n.a.	5–200 μm
Aegerine	$NaFeSi_2O_6$	3.50–3.54	n.a.	<0.4 mm
Perovskite	$CaTiO_3$	3.98–4.26	Ti	
Nb-rutile	$(Ti,Nb,Fe)O_2$	4.35–4.92	Ti, Nb	<1 mm*
Allanite	$(Ce,Ca,Y)_2(Al,Fe)_3(SiO_4)_4(OH)$	3.3–4.2	LREE, Y	1–4 mm

n.a. = not applicable; LREE = La, Ce, Pr, and Nd.
* indicates exceptionally coarse samples.

indicator mineral examination and hand-picking (Averill, 2001; McClenaghan, 2011). Traditional methods involving hand-picking indicator minerals are limited to monomineralic grains and composite grains denser than the specific gravity of the separation, typically 3.2 g/cm^3. Composite grains are recovered during hand-picking, though they may be lost during initial processing. Furthermore, texturally and mineralogically complex grains are difficult and time consuming to hand pick, visually identify, and characterize using optical methods and may require confirmation by scanning electron microscopy (SEM) methods. Picking the 0.25 to 0.5 mm fraction is particularly time consuming as this fraction is generally larger than the 0.5 to 1 and 1 to 2 mm fractions and, being finer grained, contains many more particles, ~10,000 per gram, many of which are contained within composite grains not easily identified and picked visually. For the purposes of this study, a particle is defined as a single mineral crystal. A particle can contain other mineral particle inclusions. A grain is defined as a single piece of detrital material found in the stream sediments. Several particles can be contained within a larger composite grain. A grain can also consist of a single large mineral particle.

Fully picking a typical 20 g or 200,000 grain concentrate for indicator minerals of a broad spectrum of deposit types normally requires

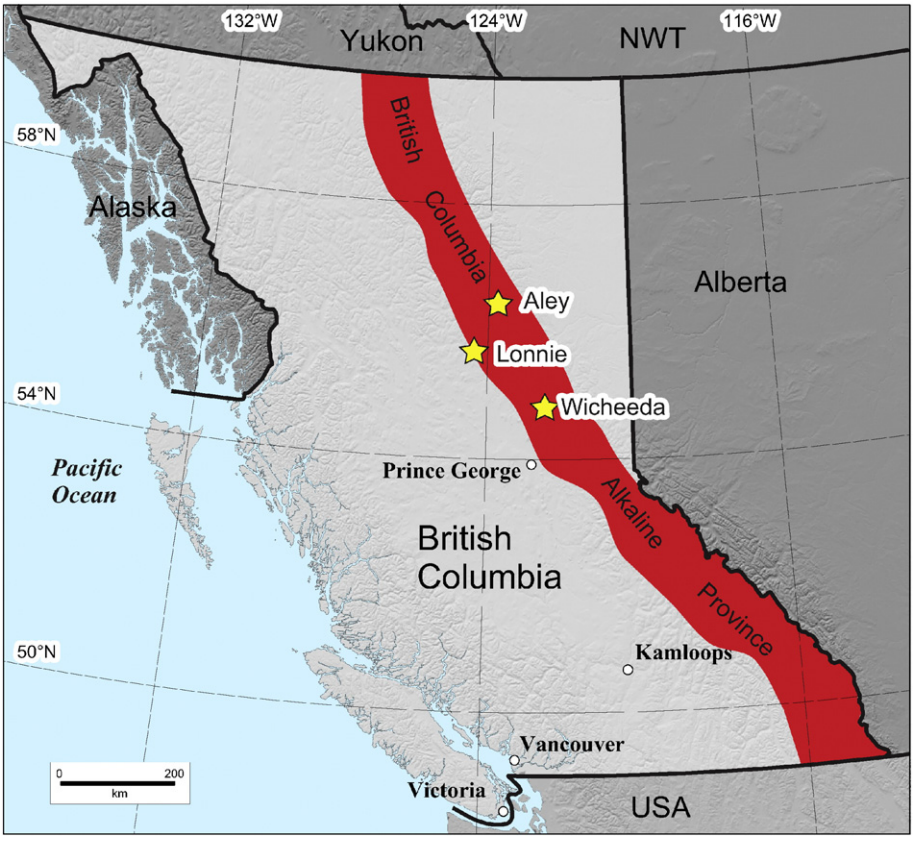

Fig. 1. Location of the Aley, Lonnie, and Wicheeda carbonatites (stars).

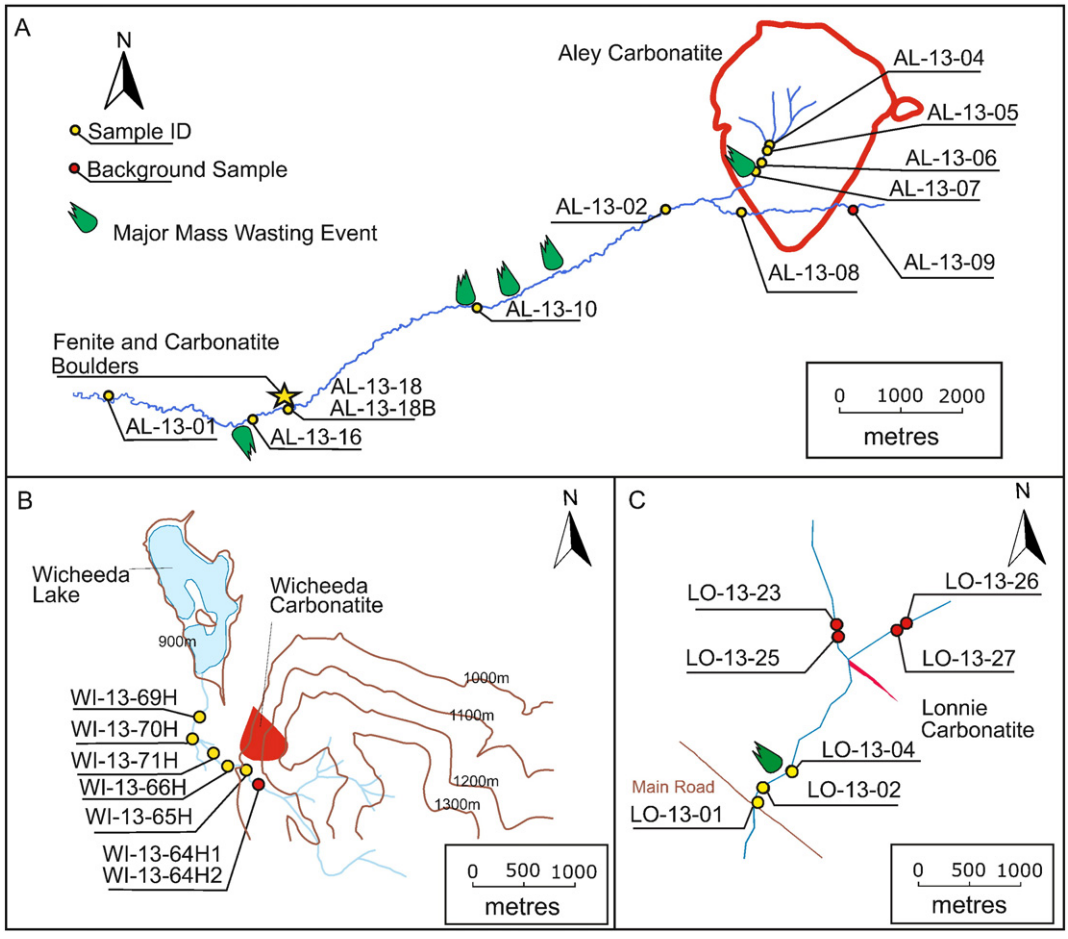

Fig. 2. Stream sediment sample location maps for the (A) Aley, (B) Wicheeda, and (C) Lonnie carbonatites. Streams draining the Aley and Lonnie carbonatites flow to the southwest; the stream draining the Wicheeda carbonatites flows to the northwest.
Modified from Luck and Simandl (2014) and Mackay and Simandl (2014b,c).

approximately 2 h as well as a few minutes for SEM checks on 1 to 5 unresolved grains (S. Averill, pers. comm., August 2015). Therefore, ~4 samples can be picked per person in a typical 8-hour day when focusing on classical indicator mineral suites (e.g. kimberlite and Au deposits). Five to ten pickers normally work together to complete up to 50 samples per day, with one also performing any required SEM checks. One epoxy grain mount containing 200 to 500 indicator mineral grains (in the 0.25 to 2 mm size fraction) selected from sediment samples can take 6–12 h to characterize and chemically analyze using traditional SEM techniques (Layton-Matthews et al., 2014). For the purposes of this study, a polished thin section was made from a split of the unprocessed material and concentrated material for the 125–250 μm size fraction of each stream sediment sample.

Detailed particle analysis using the QEMSCAN® Particle Mineral Analysis routine takes approximately 3.5–4.5 h per polished thin section or puck (containing 5000–20,000 particles). An additional 1–1.5 h is required to change sample batches. This allows for 5–6 samples to be analyzed per instrument per 24-hour day. When only mineral identification and concentration or abundance are required, the much faster Bulk Mineral Analysis routine can be used instead. This reduces the QEMSCAN® analysis time from ~4 h to ~30 min per sample (8 times faster). If subsequent transmitted light optical investigation is not required, polished pucks can be used. The sample holder for 30 mm blocks may accommodate more samples per batch (14) than the polished thin section holder (12 sections), slightly reducing turnaround time required to change batches. This allows for rapid identification of indicator minerals from complex deposits such as carbonatites. However, polishing may obscure or erase textural features and remove alteration minerals in some cases.

This study assesses the use of QEMSCAN® to provide (with no additional processing other than dry sieving) detection and characterization of indicator minerals (when found in high concentrations) from carbonatite deposits. The use of preconcentration of stream sediments by Mozley C800 separator is also investigated for low concentrations of indicator minerals.

1.1. Potential indicator minerals

Pyrochlore supergroup minerals (as defined by Atencio et al., 2010), columbite–tantalite series minerals (as defined by Černý and Ercit, 1985; Černý et al., 1992), rare earth element (REE)-bearing fluorocarbonates (such as bastnaesite and synchysite), monazite, and apatite (Bühn et al., 2001; Belousova et al., 2002a) are ideal carbonatite indicator minerals (Mackay et al., 2015a,b; Mackay and Simandl, 2015). Their chemical stability in weathered surficial sediments and high density allows for easy recovery by density separation methods while high content of key pathfinder elements such as Nb, Ta, light rare earth elements (LREE; for the purposes of this study LREE = ΣLa, Ce, Pr, and Nd), and P (Table 1) allow for indirect detection using bulk geochemical analysis (Luck and Simandl, 2014; Mackay and Simandl, 2014b,c). Indicator minerals have a broad range of sizes in all three carbonatites studied; typical and exceptional sizes for these minerals are given in Table 1. Based on bulk geochemical stream sediment orientation surveys by

Table 2
Weight of unprocessed material and Mozley concentrate with corresponding concentration factors (Mackay et al., 2015a).

Sample ID	Starting weight (g)	Concentrate weight (g)	Concentration factor
AL-13-10	88.5	24.0	3.7
AL-13-02	74.5	22.2	3.4
AL-13-05	79.5	20.1	4.0
AL-13-06	90.5	27.3	3.3
AL-13-09	65	2.5	26.2
AL-13-01	68.5	19.2	3.6
AL-13-04	73.5	20.5	3.6
AL-13-07	68.5	10.0	6.8
AL-13-08	80.5	19.9	4.0
AL-13-16-15	73.5	23.5	3.1
AL-13-18	73.5	18.4	4.0
AL-13-18B	78	23.1	3.4
LO-13-01	77.99	9.78	8.0
LO-13-02	72	10.38	6.9
LO-13-04	78.5	9.91	7.9
LO-13-23	76	8.47	9.0
LO-13-25	72.42	9.7	7.5
LO-13-26	77.17	24.07	3.2
LO-13-27	79.43	18.84	4.2
WI-13-64H1	29.13	0.62	47.0
WI-13-64H2	29.04	2.15	13.5
WI-13-65H	29.88	0.99	30.2
WI-13-66H	29.23	1.47	19.9
WI-13-69H	28.3	4.39	6.4
WI-13-70H	26.79	2.69	10.0
WI-13-71H	25.59	0.57	44.9

Luck and Simandl (2014) and Mackay and Simandl (2014b,c), the 125–250 μm size fraction was determined to be ideal for further study.

Other potential indicator minerals occur as gangue and/or as constituents of fenitized (Na–K hydrothermal alteration) zones associated with carbonatites. These include (based on the expected mineralogy of carbonatite complexes), but are not limited to: magnetite, zircon (Belousova et al., 2002b), barite–celestine series minerals, Na-pyroxenes (e.g. aegirine), Na and K amphiboles (e.g. arfvedsonite and richterite), fluorite (Makin et al., 2014), Nb-rutile, baddeleyite, perovskite, and allanite (Lehtonen et al., 2011). There are very few studies focusing on the identification of indicator minerals for carbonatites and related deposits (Vartiainen, 1976; Lehtonen et al., 2011; Makin et al., 2014; Mao et al., 2015a,b).

1.2. Geological setting and characterization of carbonatite-related deposits in British Columbia

Three carbonatites in the British Columbia Alkaline Province (Pell, 1994) were selected for indicator mineral studies. The Aley carbonatite (a large, high-grade Nb-deposit) is located 290 km north of Prince George, British Columbia (Fig. 1). The Aley carbonatite outcrops intermittently over an area 3 to 3.5 km in diameter (Fig. 2; Mäder, 1986). The area was glaciated most recently during the last glacial maximum. The carbonatite is located in a U-shaped glacial valley. A small creek, and seasonal tributary creeks, flow over the carbonatite. Glacial distribution of indicator minerals is possible but is outside of the scope of this study. Boreal forest covers the area below ~1600 m; the central portion of the deposit is dominated by alpine shrubs and grasses and thin till and soil cover (~1 m where observed).

The Aley carbonatite is the largest and most important Nb-deposit in the Canadian Cordillera. It has a measured plus indicated resource of 286 million tonnes at 0.37 wt.% Nb_2O_5, with a cut-off grade of 0.20 wt.% Nb_2O_5 (Jones et al., 2014). This deposit has low REE content relative to other carbonatites (Simandl et al., 2014). Deposit geology is described by Mäder (1986); Kressall et al. (2010); McLeish (2013), and Mackay and Simandl (2014b).

The Lonnie carbonatite (a relatively small, low grade Nb showing) is located 220 km northwest of Prince George (Fig. 1) and occurs as an

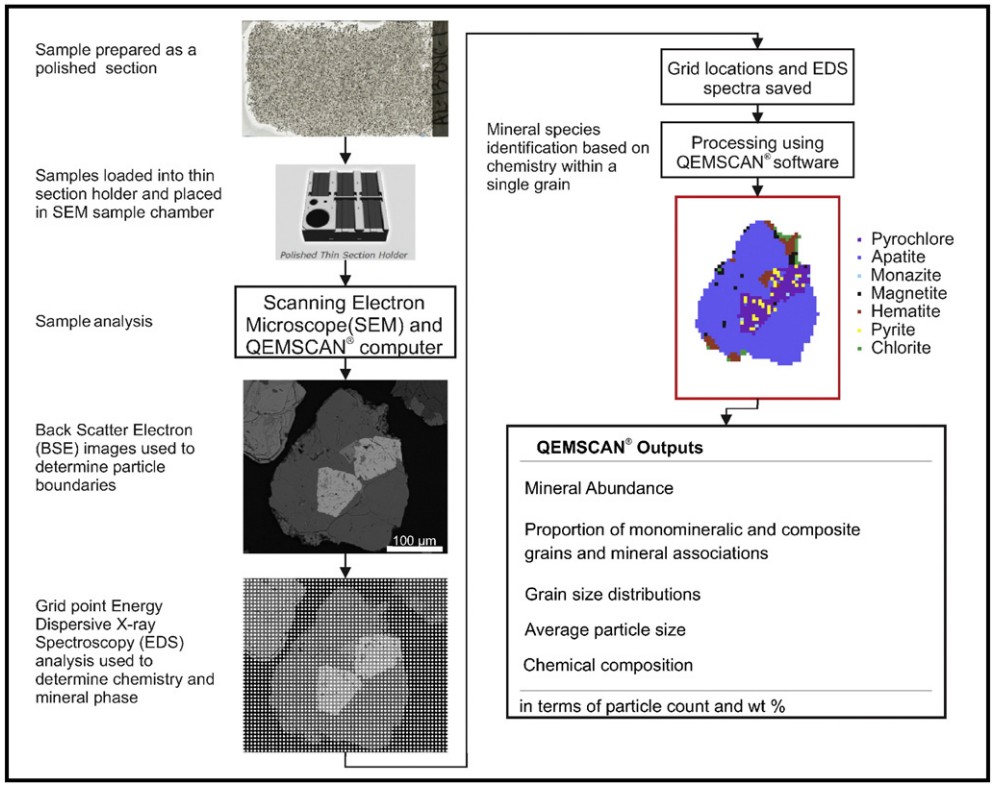

Fig. 3. Flow chart for QEMSCAN® analysis using the Particle Mineral Analysis routine. Based on QEMSCAN® software help file. Example grain is a polymineralic, or composite grain, with seven different mineral phases (identified in red box).

Table 3
Indicator mineral concentrations (wt.%) in the RAW stream sediment samples and Mozley concentrates (CON) from the Aley (AL), Lonnie (LO), and Wicheeda (WI) carbonatites. Mineral abbreviations: pyrochlore (Pcl); columbite-(Fe) (Cmb); fersmite (Fer); REE-fluorocarbonates (REE-Fl); zircon (Zrc); apatite (Ap); magnetite (Mag); hematite (Hem); rutile (Rt); amphibole/pyroxene (Amp/Px); and barite (Brt).

Sample ID	Pcl	Cmb	Fer	Mnz	REE-Fl	Zrc	Ap	Mag	Hem	Rt	Amp/Px	Brt
AL-13-01 RAW	0.64	0.32	0.01	0.63	0.07	0.14	6.22	2.03	5.18	0.14	1.49	0.16
AL-13-01 CON	1.42	1.36	0.04	1.45	0.32	0.36	13.10	3.76	12.73	0.24	1.42	0.26
AL-13-02 CON	1.82	2.07	0.05	3.38	0.47	0.54	17.47	3.67	22.14	0.19	1.00	0.01
AL-13-04 RAW	0.11	1.88	0.26	0.49	0.31	0.08	19.26	0.67	13.54	0.15	2.73	0.01
AL-13-04 CON	2.17	3.02	0.06	1.92	0.25	0.35	27.40	7.07	19.21	0.20	2.25	0.01
AL-13-10 CON	2.07	2.01	0.05	2.51	0.67	0.52	15.60	12.08	10.88	0.32	1.31	0.11
AL-13-16 RAW	0.06	0.87	0.35	0.47	0.17	0.17	6.42	1.29	8.51	0.13	1.12	0.14
AL-13-16 CON	1.02	1.12	0.04	1.61	0.38	0.41	10.66	6.16	6.68	0.18	1.69	0.06
LO-13-01 RAW	n.d.	0.01	0.00	0.11	0.01	0.08	0.46	0.03	0.35	0.47	3.30	0.00
LO-13-01 CON	0.01	0.06	0.00	0.21	0.04	0.27	1.23	0.17	0.66	1.25	6.09	0.00
LO-13-02 RAW	0.00	0.01	0.01	0.05	0.01	0.14	0.47	0.07	0.32	0.35	2.70	0.01
LO-13-02 CON	0.01	0.04	0.00	0.22	0.04	0.16	0.86	0.12	0.44	1.05	4.79	0.00
LO-13-25RAW	n.d.	0.00	0.00	0.05	n.d.	0.07	0.40	0.00	0.28	0.29	3.41	0.00
LO-13-25 CON	0.02	0.04	0.00	0.35	0.03	0.15	1.39	0.03	0.57	0.75	5.30	0.00
WI-13-64H2 RAW	0.00	0.00	0.02	0.25	0.12	0.04	0.23	0.06	2.70	0.42	2.52	0.02
WI-13-64H2 CON	0.01	0.02	0.05	2.01	1.56	0.20	0.70	0.79	15.13	2.77	2.00	0.11
WI-13-69H RAW	0.00	0.00	0.01	0.48	0.48	0.05	0.42	0.05	3.87	0.94	1.63	0.04
WI-13-69H CON	0.00	0.04	0.05	1.50	0.97	0.08	0.61	0.50	9.23	2.19	2.17	0.05
WI-13-70H RAW	0.00	0.04	0.02	0.43	0.58	0.08	0.35	0.05	3.23	0.76	1.53	0.06
WI-13-70H CON	0.01	0.09	0.07	2.74	1.37	0.17	0.57	1.48	10.65	2.45	1.72	0.05

n.d. = not detected.

Table 4
Indicator mineral concentrations (mineral count) for the RAW stream sediment samples and corresponding Mozley concentrates (CON) from the Aley (AL), Lonnie (LO), and Wicheeda (WI) carbonatites. Mineral abbreviations are the same as Table 2.

Sample ID	Pcl	Cmb	Fer	Mnz	REE-Fl	Zrc	Ap	Mag	Hem	Rt	Amp/Px	Brt	Total
AL-13-01 RAW	121	65	130	317	88	123	2526	309	789	1448	6219	24	19,994
AL-13-01 CON	353	227	327	679	157	233	4356	851	1717	1233	3635	57	13,700
AL-13-02 CON	489	375	443	1029	224	297	5195	891	2298	1110	3053	43	13,114
AL-13-04 RAW	177	456	323	453	145	81	5328	348	1951	858	3541	32	19,374
AL-13-04 CON	707	593	654	1178	168	305	9910	1096	3342	1188	3769	65	16,908
AL-13-10 CON	660	478	639	1529	560	408	6763	2269	2674	1523	4364	75	24,525
AL-13-16 RAW	105	222	167	271	77	119	2605	420	1039	1405	5386	26	18,797
AL-13-16 CON	335	227	323	668	162	167	4850	795	1563	1043	5961	34	18,912
LO-13-01 RAW	0	2	8	44	6	92	356	23	190	1116	3606	2	22,017
LO-13-01 CON	10	9	11	73	11	146	637	69	298	2112	4761	5	30,752
LO-13-02 RAW	2	6	5	27	6	80	268	26	203	847	2631	1	15,596
LO-13-02 CON	3	1	17	62	12	103	598	53	259	1665	4780	33	34,602
LO-13-25RAW	0	3	9	17	0	100	160	7	141	451	1534	2	11,483
LO-13-25 CON	10	14	10	73	9	138	553	41	176	1119	2675	1	21,337
WI-13-64H2 RAW	4	8	59	145	37	196	952	55	815	3504	12,009	57	44,992
WI-13-64H2 CON	33	37	233	488	311	181	894	544	2262	3902	7414	11	24,294
WI-13-69H RAW	11	26	51	159	59	186	912	72	728	2972	4828	36	19,270
WI-13-69H CON	26	29	182	324	173	180	917	321	1257	3681	6013	3	21,805
WI-13-70H RAW	5	22	45	143	60	161	924	53	652	2806	4862	0	19,805
WI-13-70H CON	19	57	246	469	245	187	852	523	1556	3459	5911	20	21,315

elongate 650 m by 50 m intrusive body dipping 60° to the southwest (Fig. 2; Hankinson, 1958; Rowe, 1958). The carbonatite outcrops sporadically along the occurrence and is covered by till and soil ≥30 cm thick. A small creek (Granite Creek) is located downslope of much of the Lonnie carbonatite and flows over the lower portion. Trenching delineated a zone ~530 m long and ~17 m wide grading 0.21 wt.% Nb_2O_5 (Rowe, 1958; Chisholm, 1960). Geology is described in detail by Simandl et al. (2013) and Luck and Simandl (2014).

The Wicheeda carbonatite (a small, high-grade LREE deposit) is located 85 km northeast of Prince George (Fig. 1). The drilled portion of the deposit is sub-circular in plan view and >250 m in diameter with sparse outcrop exposure (Fig. 2; Mackay and Simandl, 2014c; Trofanenko et al., 2014). The carbonatite is overlain by a red soil or regolith horizon characteristic of carbonatites which is 5 cm to more than 50 cm thick. A small stream (unnamed) is located just downhill of the carbonatite exposure. The area was also glaciated during the last glacial maximum. Drilling intersected high-grade zones consisting of 3.55 wt.% total rare earth oxides (TREO) over 48.6 m, 2.2 wt.% over 144 m, and 2.9 wt.% over 72 m (Graf et al., 2009; Lane, 2009). Deposit geology is described in detail by Graf et al. (2009), Lane (2009), and Trofanenko et al. (2014).

Table 5
Concentration of Nb, LREE, and Fe_2O_3 in polished smear sections determined by QEMSCAN®.

Sample ID	Fe_2O_3 (wt.%)	Nb (ppm)	LREE (ppm)
AL-13-01 RAW	8.9	5189	2451
AL-13-04 RAW	17.5	11,935	3305
AL-13-16 RAW	11.6	6503	3620
AL-13-01 C	18.4	15,106	4614
AL-13-02 C	28.2	21,141	13,051
AL-13-04 C	29.5	28,214	10,570
AL-13-10 C	25.4	22,139	11,829
AL-13-16 C	14.9	11,696	10,270

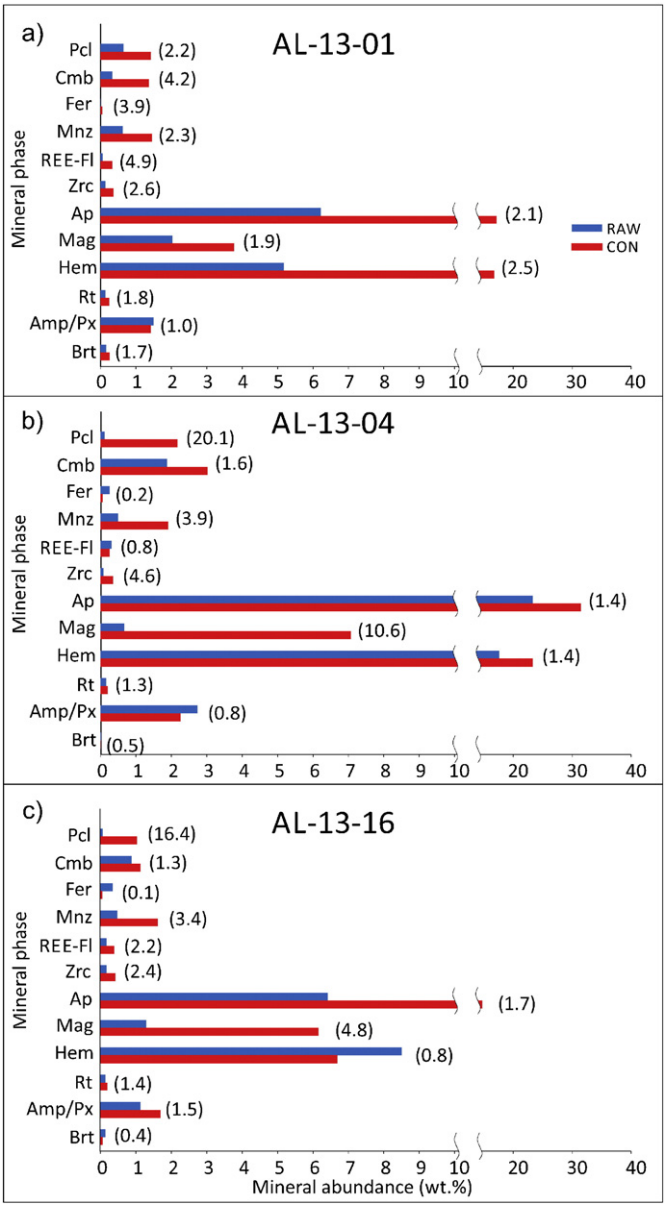

Fig. 4. Mineral abundance (wt.%; determined by QEMSCAN®) for RAW and corresponding Mozley C800 concentrates (CON) for selected samples a) AL-13-01, b) AL-13-04, and c) AL-13-16. Concentration factors for CON relative to corresponding unprocessed (RAW) samples are shown in parentheses. Mineral abbreviations are the same as in Table 2.

2. Methodology

2.1. Sampling, portable XRF analysis, and sample processing

The samples collected for this study consist of coarse grained through sand sized fluvial sediments collected in the field and pre-sieved to <8 mm material. Material along stream banks and in the lee of logs and boulders were preferentially targeted (Luck and Simandl, 2014; Mackay and Simandl, 2014b,c). A total of 12 samples (weighing 4.1 to 21.8 kg) from the Aley drainage were collected for this study over 11 km as access to the river allowed, with 7 from Lonnie over 3 km as access allowed (weighing 3.7 to 16.1 kg), and 7 from Wicheeda over 1.5 km with 150–200 m spacing (weighing 1.1 to 5.4 kg; Fig. 2; Luck and Simandl, 2014; Mackay and Simandl, 2014b,c). One sample from Aley (AL-13-09) was collected upstream of the deposit to assess indicator mineral background in the area, though insufficient material was recovered following Mozley processing for complete analysis of

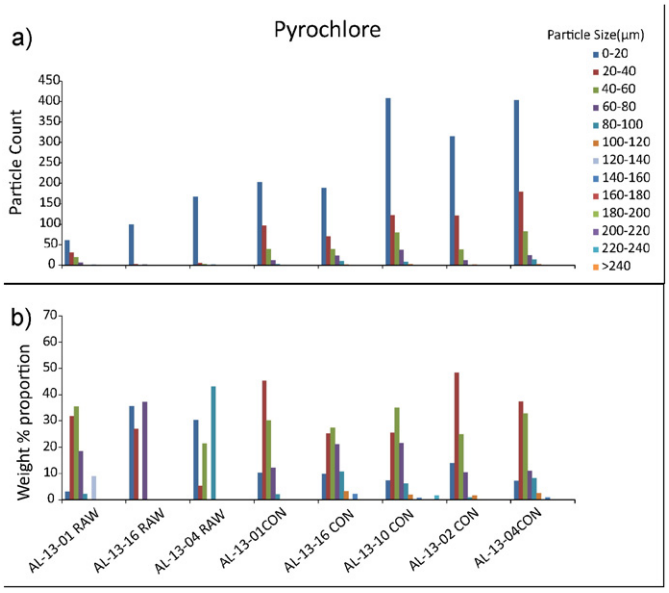

Fig. 5. Particle size distribution for pyrochlore in terms of (a) mineral count and (b) wt.%. RAW samples and corresponding Mozley concentrates (CON) samples are each ordered from west (away from the deposit) to east (nearest the deposit). Mineral sizes are in μm.

the concentrate. Samples LO-13-23, LO-13-25, LO-13-25, and LO-13-27 were collected upstream of the Lonnie carbonatite to assess background indicator mineral abundance. Samples WI-13-64H1 and WI-13-64H2 were collected upstream of the Wicheeda carbonatite as background samples.

Samples were dried and sieved into +4 mm, 2 mm to 4 mm, 1 mm to 2 mm, 500 μm to 1 mm, 250 μm to 500 μm, 125 μm to 250 μm, 63 μm to 125 μm, and −63 μm size fractions using stainless steel sieves (cleaned using a stiff brush and ultrasonic bath). Each size fraction passed through a riffle-type splitter. Part of the sample was kept as a witness; the remainder was further split for pXRF analyses. Sample locations, sampling methodology, sample processing, and indicator

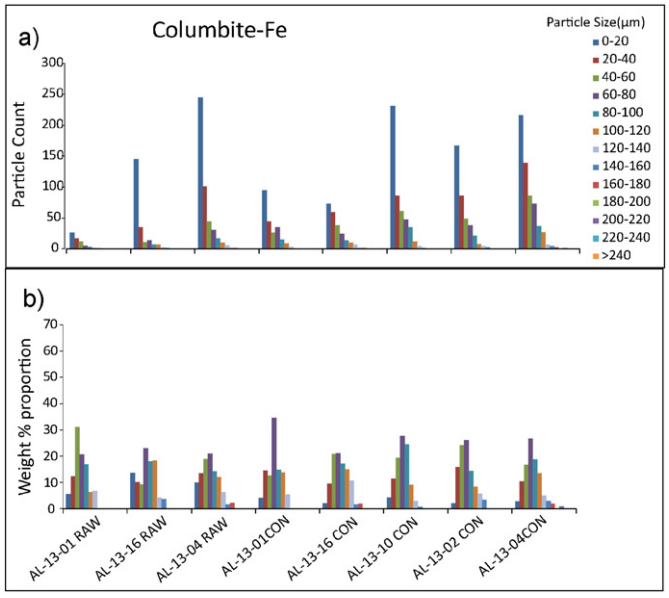

Fig. 6. Particle size distribution for columbite-(Fe) in terms of (a) mineral count and (b) wt.%. RAW samples and corresponding Mozley concentrates (CON) samples are each ordered from west (away from the deposit) to east (nearest the deposit). Mineral sizes are in μm.

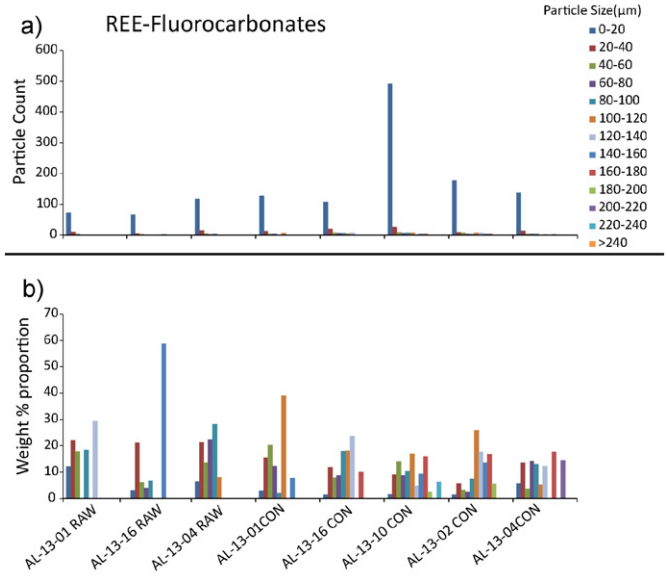

Fig. 7. Particle size distribution for REE-fluorocarbonates in terms of (a) mineral count and (b) wt.%. RAW samples and corresponding Mozley concentrates (CON) samples are each ordered from west (away from the deposit) to east (nearest the deposit). Mineral sizes are in μm.

mineral recovery methods are fully described by Luck and Simandl (2014) and Mackay and Simandl (2014b,c).

Within carbonatites, Nb is predominantly incorporated in pyrochlore and columbite-(Fe); LREE in REE-fluorocarbonates; LREE, P, Th, Y in monazite; and P in apatite (Table 1; Linnen et al., 2014; Chakhmouradian et al., 2015). High concentrations of Nb, LREE, and P were detected in unprocessed stream sediments by portable X-ray fluorescence (pXRF; Luck and Simandl, 2014; Mackay and Simandl, 2014b, c) and traditional chemical analyses. Mineral size distribution analysis of carbonatite pathfinder elements (Nb, Ta, LREE, Y, P, Ba, Sr, U, and Th) in stream sediments downstream from the three carbonatites led to the selection of the 125–250 μm dry sieved fine sand fraction (herein referred to as raw or unprocessed) as optimal for carbonatite indicator

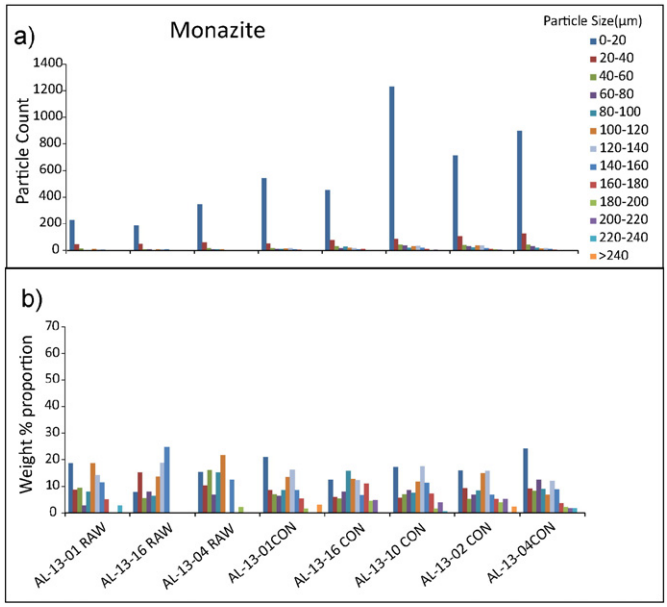

Fig. 8. Particle size distribution for monazite in terms of (a) mineral count and (b) wt.%. RAW samples and corresponding Mozley concentrates (CON) samples are each ordered from west (away from the deposit) to east (nearest the deposit). Mineral sizes are in μm.

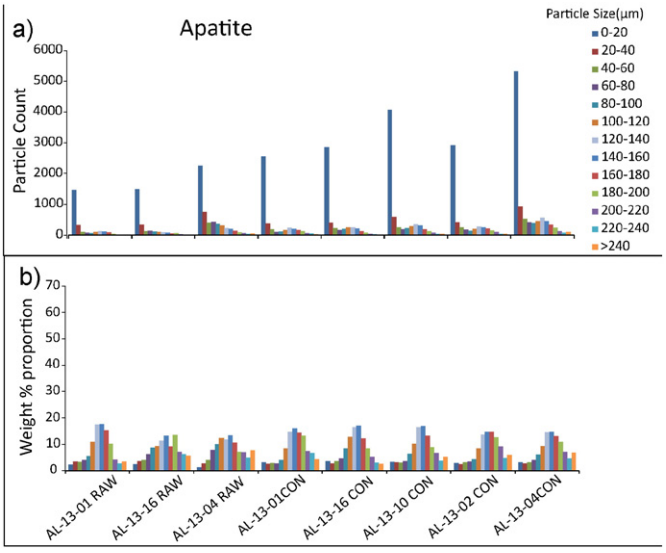

Fig. 9. Particle size distribution for apatite in terms of (a) mineral count and (b) wt.%. RAW samples and corresponding Mozley concentrates (CON) samples are each ordered from west (away from the deposit) to east (nearest the deposit). Mineral sizes are in μm.

mineral studies (Luck and Simandl, 2014; Mackay and Simandl, 2014b,c). All materials used in this study are from the 125–250 μm size fraction.

The high pathfinder element concentrations (determined by pXRF) in stream sediments directly over and downstream of the Aley carbonatite (Mackay and Simandl, 2014b) and elevated grade of mineralization in this carbonatite (Kressall et al., 2010; Jones et al., 2014) gave the expectation that indicator minerals would be detectable by QEMSCAN®. However, pathfinder element levels were much lower in sediments downstream from Lonnie and Wicheeda (Luck and Simandl, 2014; Mackay and Simandl, 2014c), necessitating preconcentration by gravity concentration of stream sediments to increase indicator mineral levels prior to analysis. Previous studies showed that the Wilfley #13 shaking table and Mozley C800 laboratory mineral separator consistently concentrated the targeted indicator minerals (Mackay et al., 2015a,b). The Mozley table is more suitable for processing small samples (50–75 g versus kilograms of material) such as those presented in this study. The optimized processing procedure for the Mozley table is described by Mackay et al. (2015b). The Mozley C800 operates by gently washing material using water and an oscillating sloped tray. Optimization of the Mozley procedure using a synthetic concentrate composed of quartz, fluorite, garnet, and magnetite was used to target material denser than almandine garnet (>4.1 g/cm^3; Mackay et al., 2015a). The typical concentration ratio was 3.1–26.2 (average 5.8) at Aley, 3.2–9.0 (average 6.7) at Lonnie, and 6.4–47.0 (average 24.6) at Wicheeda (Table 2); i.e. the indicator minerals were concentrated a number of times equal to the concentration factor relative to their abundance in the raw sample. While great care was taken in optimization of the concentration process, minor amounts of less dense indicator minerals such as fluorite and apatite may have been lost during processing. This may have a minor effect the final indicator mineral ratio of concentrates. This study was optimized to capture denser minerals more suited to carbonatite exploration such as pyrochlore and columbite. No heavy liquids or isodynamic separation were used.

2.2. QEMSCAN® methods

Approximately 2 g of unprocessed sample or corresponding Mozley C800 concentrate (equivalent to ~20,000 grains) were mounted on each 26 × 46 mm polished smear sections for QEMSCAN analysis (Fig. 3). A total of 3 unprocessed samples and 5 concentrates were analyzed from Aley stream sediments, as well as 3 unprocessed and 3 concentrates from Lonnie and Wicheeda. Analysis of the grain mounts was

Table 6
Chemical analysis of the RAW stream sediments and corresponding Mozley concentrates (CON) from the Aley carbonatite drainage area.

Sample ID	AL-13-01 RAW	AL-13-02 RAW	AL-13-04 RAW	AL-13-10 RAW	AL-13-16 RAW	AL-13-18 RAW	AL-13-01 CON	AL-13-02 CON	AL-13-04 CON	AL-13-10 CON	AL-13-16 CON
Major oxides (wt.%)											
SiO_2	30.00	23.60	7.30	25.90	28.90	30.10	14.90	6.35	3.85	8.04	14.00
Al_2O_3	3.68	3.10	1.04	3.47	3.61	3.85	1.67	0.76	0.55	0.90	1.50
Fe_2O_3	5.43	10.50	11.90	8.96	7.86	5.76	12.70	27.30	25.60	22.30	18.35
CaO	21.10	23.20	28.20	22.70	20.40	21.60	26.00	22.40	25.80	23.70	22.20
MgO	8.97	7.65	12.05	8.91	8.83	9.24	10.05	6.81	6.24	7.80	8.38
Na_2O	0.24	0.24	0.25	0.21	0.26	0.28	0.19	0.12	0.20	0.15	0.16
K_2O	1.11	1.16	0.19	1.17	1.15	1.24	0.42	0.26	0.16	0.28	0.44
TiO_2	0.32	0.39	0.40	0.38	0.38	0.33	0.53	0.70	0.73	0.64	0.61
MnO	0.14	0.21	0.48	0.19	0.16	0.16	0.19	0.24	0.32	0.23	0.18
P_2O_5	2.48	3.57	8.21	3.35	2.75	2.52	6.32	7.94	12.10	7.36	5.46
SrO	0.09	0.14	0.26	0.12	0.09	0.09	0.13	0.17	0.24	0.16	0.12
BaO	0.07	0.03	0.02	0.04	0.10	0.08	0.10	0.03	0.02	0.06	0.15
LOI	24.40	24.00	27.80	24.80	23.80	24.80	25.00	18.05	15.30	20.90	22.30
Trace elements (ppm)											
Nb	3700	7400	10,000	5800	5500	3000	11,900	22,400	25,900	17,700	15,200
Ta	55	109	89	82	80	52	184	255	124	197	217
Ba	672	242	196	395	883	713	915	241	175	532	1400
Zr	424	912	849	765	680	459	1180	2800	2290	2100	1745
Hf	7	14	14	12	10	7	18	40	37	31	26
U	19	34	24	30	27	18	61	103	64	86	74
Th	137	267	324	206	189	134	450	786	723	615	522
La	576	1705	1430	1220	1015	658	1715	5150	3320	3560	2790
Ce	922	2650	2480	1900	1605	1065	2740	7880	5560	5560	4350
Pr	90	260	258	180	154	102	281	750	569	539	424
Nd	308	816	863	601	511	341	904	2470	1980	1805	1385
Sm	44	96	123	78	68	47	127	291	255	216	172
Eu	10	24	29	18	15	11	31	65	60	49	40
Gd	27	57	74	44	39	28	79	155	148	120	98
Tb	3	7	9	5	5	4	10	18	18	14	12
Dy	16	31	42	25	22	16	46	83	82	64	55
Ho	3	5	7	4	3	3	8	13	13	10	9
Er	7	12	16	10	8	6	18	31	31	24	21
Tm	1	1	2	1	1	1	2	4	3	3	2
Yb	4	8	10	6	5	4	11	19	18	14	13
Lu	1	1	1	1	1	0	1	2	2	2	2
Y	70	127	167	102	91	70	189	345	344	272	232
Rb	30	27	6	28	30	33	11	5	3	6	11
Sr	799	1275	2290	1075	839	857	1275	1630	2280	1535	1175
V	136	218	155	183	182	155	175	399	333	334	282
W	182	114	43	130	147	136	247	147	167	210	274
Sn	5	10	14	8	7	5	14	28	32	23	19
Cs	1	1	0	1	1	1	0	0	0	0	0
Ga	9	16	15	13	13	10	15	38	29	29	23
Total	99.11	99.94	100.68	101.89	99.88	101.08	101.19	97.20	97.07	97.22	97.88

performed using an automated FEI Quanta scanning electron microscope (SEM) with a tungsten filament operating at 10.00 nA and a maximum voltage of 25 keV. The QEMSCAN® procedure and IDiscover® software were used to collect and process data.

The automated QEMSCAN® Particle Mineral Analysis routine acquires a back scatter electron (BSE) image of each grain in which the minerals are differentiable by contrast in brightness, reflecting their different densities (Fig. 3). Energy dispersive X-ray spectroscopy (EDS) analysis, performed on a grid (6.5 μm spacing in this study), provides chemical composition and identifies each mineral based on a customized Species Identification Protocol. Mineral abundance in weight percent (wt.%) is calculated using particle volume (based on the polished surface area) and density of the identified mineral particle. In addition to mineral wt.%, QEMSCAN® analysis output includes particle count, particle size distribution(s), chemistry, and proportion of monomineralic (i.e. completely liberated) and composite grains (complex polymineralic grains) with mineral associations (Fig. 3). QEMSCAN® bulk chemical composition is derived from the chemical compositions of the mineral particles determined by EDS, volume measurements (which assume the composition of the polished section is representative of the entire particle in three dimensions and each particle is uniform in shape), and idealized mineral densities. Two of the five samples from the Aley area had insufficient raw sediments.

2.3. Chemical analysis

To determine the concentration of pathfinder elements a 3.5–10.5 g split of each raw sample and corresponding Mozley concentrates was analyzed using lithium metaborate fusion followed by nitric acid digestion and by inductively coupled plasma mass spectrometry (ICP-MS) for trace elements, inductively coupled plasma atomic emission spectroscopy (ICP-AES) for major elements (reported as their common oxides), and fused disk X-ray fluorescence (XRF) for Nb concentrations of >2500 ppm. However, the three Wicheeda samples were not analyzed because insufficient material remained after the samples were tabled.

3. Results

3.1. QEMSCAN®

Mineral abundance by weight percent (Table 3) and mineral count (Table 4) for each polished smear section was determined using QEMSCAN® analysis. Concentrations of Fe_2O_3, Nb, and LREE (ΣLa, Ce,

Table 7
Chemical analysis of the RAW stream sediments and corresponding Mozley concentrates (CON) from the Lonnie carbonatite drainage area.

Sample ID	LO-13-01 RAW	LO-13-02 RAW	LO-13-25 RAW	LO-13-01 CON	LO-13-02 CON	LO-13-25 CON
Major oxides (wt.%)						
SiO_2	80.20	77.10	79.70	71.40	72.90	73.10
Al_2O_3	9.78	10.25	9.71	9.89	10.10	10.50
Fe_2O_3	2.46	2.92	2.59	5.52	5.46	5.72
CaO	1.88	1.78	1.88	3.47	2.79	2.87
MgO	0.84	0.94	0.79	1.31	1.07	1.27
Na_2O	2.32	2.22	2.30	2.06	2.13	2.05
K_2O	1.48	1.60	1.47	1.02	1.11	1.30
TiO_2	0.55	0.59	0.50	1.95	1.72	1.37
MnO	0.08	0.11	0.15	0.32	0.37	0.46
P_2O_5	0.19	0.19	0.25	0.56	0.47	0.58
SrO	0.02	0.02	0.02	0.03	0.02	0.02
BaO	0.04	0.04	0.03	0.03	0.03	0.03
LOI	1.73	2.51	1.49	1.87	1.98	1.71
Total	101.58	100.28	100.89	99.46	100.17	101.00
Trace elements (ppm)						
Nb	50	70	39	235	290	192
Ta	2	3	2	7	10	7
Ba	332	345	280	285	267	263
Zr	155	195	230	531	576	553
Hf	4	5	6	12	13	13
U	3	4	7	12	15	19
Th	11	16	37	50	77	118
La	68	93	92	324	404	305
Ce	115	154	179	522	643	570
Pr	11	15	20	50	62	61
Nd	40	52	74	167	210	222
Sm	7	9	16	27	35	46
Eu	1	1	1	3	3	3
Gd	5	6	12	20	26	36
Tb	1	1	2	3	4	6
Dy	5	6	11	19	24	32
Ho	1	1	2	4	5	6
Er	3	4	7	12	15	19
Tm	0	1	1	2	2	3
Yb	3	4	6	12	14	18
Lu	0	0	1	2	2	3
Y	26	34	63	111	142	180
Rb	55	64	51	37	41	45
Sr	192	189	164	261	215	175
V	40	43	32	72	58	52
W	946	802	1150	2410	2400	2400
Sn	2	2	2	5	3	3
Cs	1	2	1	1	1	1
Ga	10	12	10	12	13	13
Total	101.58	100.28	100.89	99.46	100.17	101

Pr, Nd) of each polished smear section from Aley were determined by QEMSCAN® analysis (Table 5).

3.1.1. Aley indicator mineral abundance

All carbonatite indicator minerals were detected in raw stream sediment samples from the Aley carbonatite (Tables 3 and 4; Fig. 4). Following tabling, pyrochlore abundance increased on average by 12.9×, columbite-(Fe) by 2.4×, monazite by 3.2×, REE-fluorocarbonates by 2.6×, apatite by 1.7×, magnetite by 5.8×, and zircon by 3.2× (Table 4). Comparable increases in pathfinder element concentrations were observed during the earlier mineral concentrator optimization studies (Mackay et al., 2015b). This demonstrates effective concentration of indicator minerals by Mozley processing. The wide variation in degree of enrichment between minerals in the table concentrates largely reflects their different densities (Table 1). For example, recovery of high-density pyrochlore (S.G. 4.2–6.4) was ~8 times that for lower-density apatite (S.G. 3.16–3.22).

3.1.2. Lonnie mineral abundances

The average abundance of mineral particles in the Mozley concentrates: columbite-(Fe) by 41.2×, monazite by 4.8×, apatite by 2.7×, magnetite by 8.2×, zircon by 2.3×, and rutile by 2.8× in Mozley concentrates (Table 4).

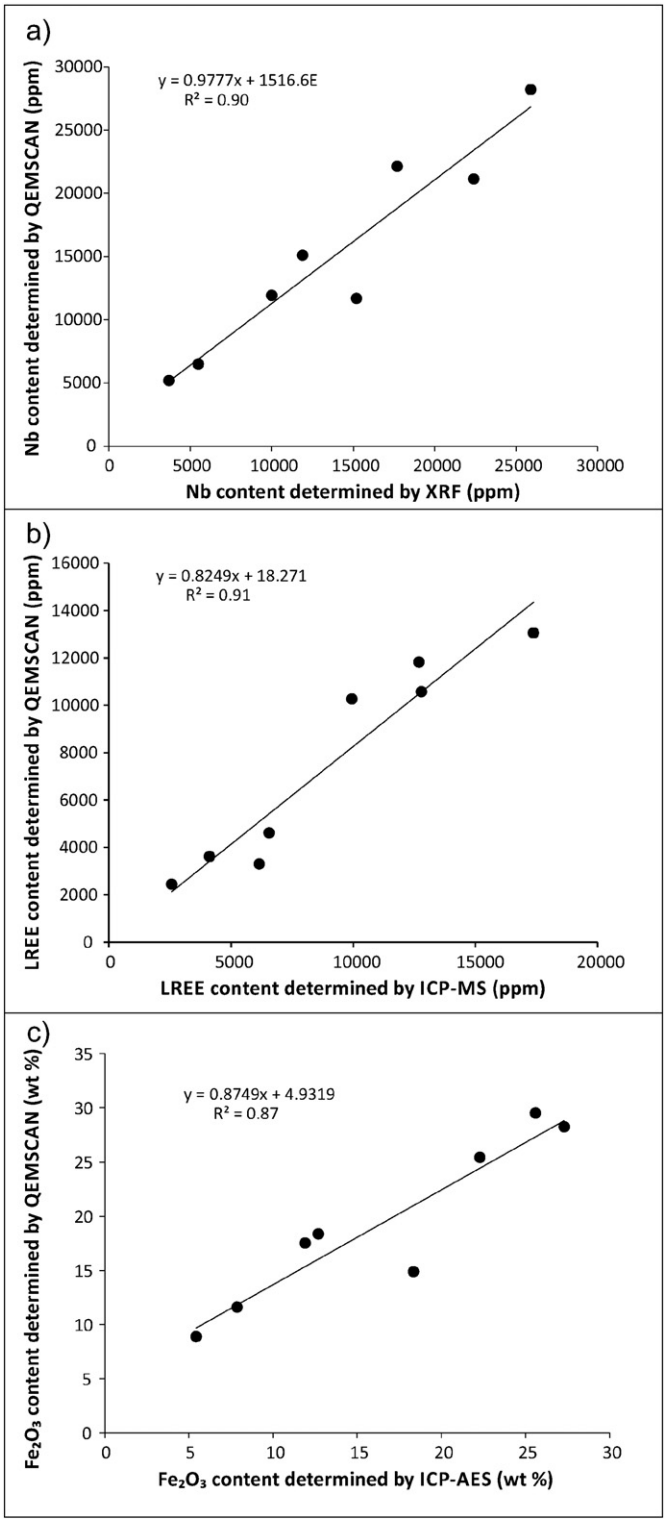

Fig. 10. Comparison of a) Nb, b) LREE, and c) Fe_2O_3 content of stream sediments from the Aley drainage area, determined by QEMSCAN® and traditional chemical analysis.

3.1.3. Wicheeda mineral abundances

The average abundance of pyrochlore in the concentrate increased by 9.0×, columbite-(Fe) by 10.7×, monazite by 5.9×, apatite by 2.0×, magnetite by 17.4×, zircon by 2.8×, and rutile by 4.1× (Table 3).

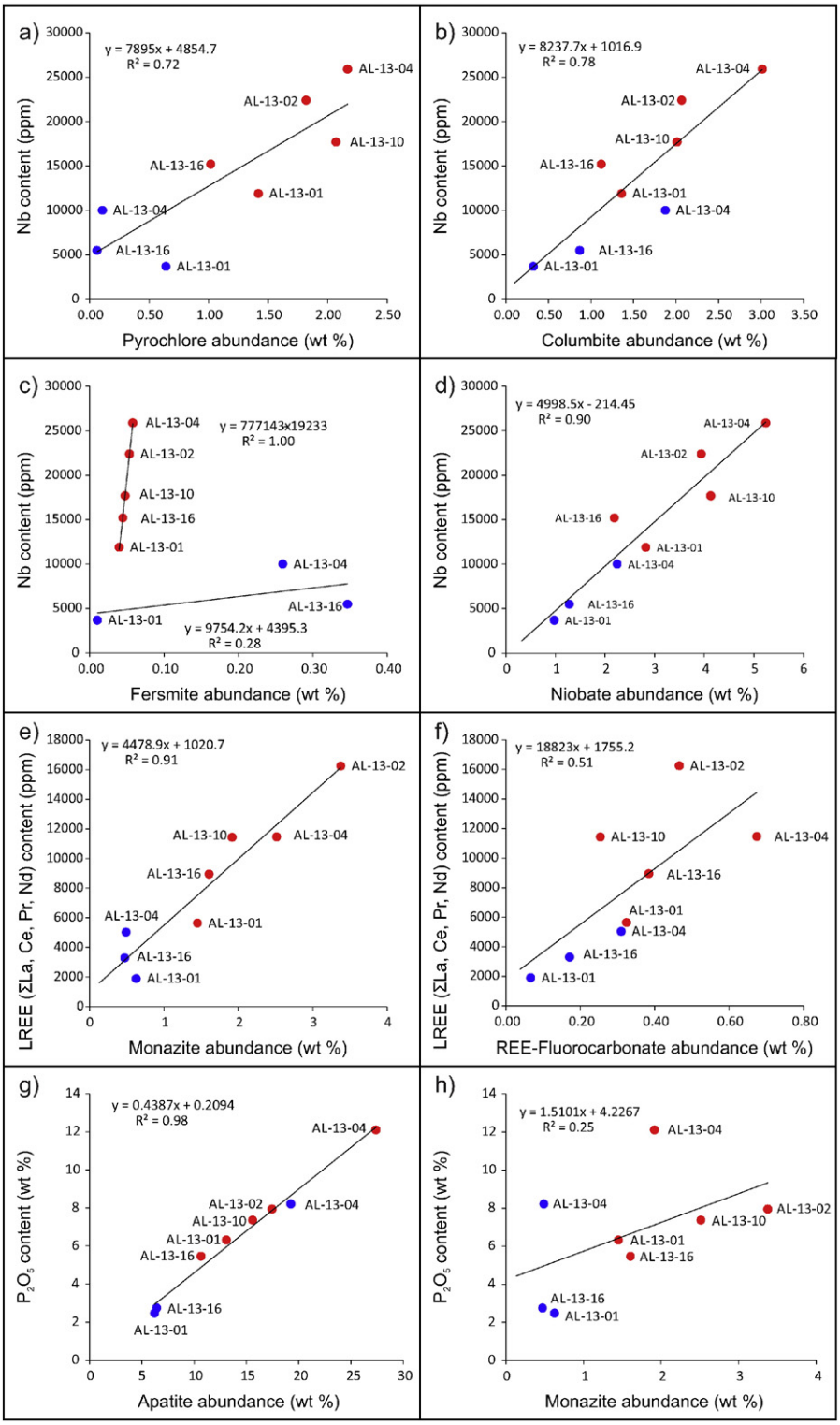

Fig. 11. Relationship between indicator mineral concentrations (determined by QEMSCAN®) and corresponding pathfinder element content for: a) Nb vs. pyrochlore; b) Nb vs. columbite(Fe); c) Nb vs. fersmite; d) Nb vs. niobates (includes pyrochlore, columbite-(Fe), and fersmite); e) LREE vs. monazite; f) LREE vs. REE-fluorocarbonates; g) P_2O_5 vs. apatite; and h) P_2O_5 vs. monazite. Results are for unprocessed samples (blue circles) and Mozley C800 concentrates (red circles).

3.1.4. Aley particle size distribution

In the three raw 125 to 250 μm fractions and five table concentrates from the Aley samples, the indicator mineral particle sizes measured by mineral count are skewed towards the smallest particles (0–20 μm; Figs. 5, 6, 7, 8, and 9). Monazite and REE-fluorocarbonates are heavily skewed towards small mineral sizes, while pyrochlore and columbite-(Fe) are commonly found as larger particles. The fine bias is most likely due to the QEMSCAN© routine identifying small indicator mineral inclusions within composite grains. When measured as weight percent, the mineral size ranges for pyrochlore, columbite-(Fe), and apatite in both the raw samples and Mozley C800 concentrates show a comparatively normal size distribution (Figs. 5b, 6b, and 9b) while REE-

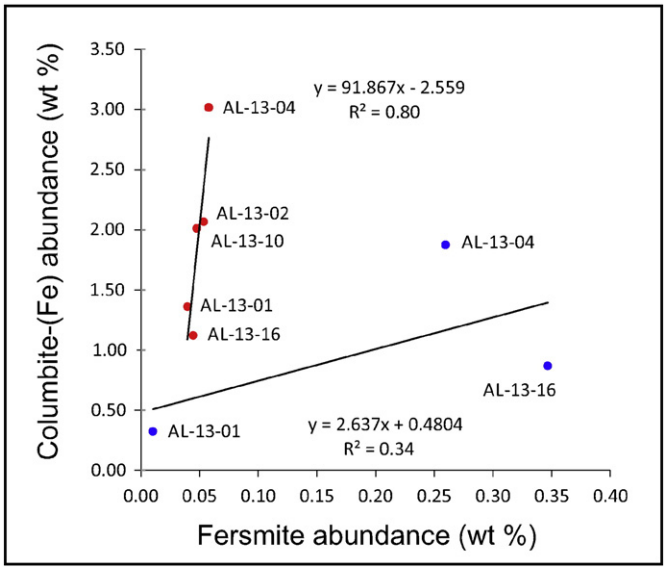

Fig. 12. Comparison of columbite-(Fe) and fersmite concentrations (determined by QEMSCAN®) for RAW (blue circles) and corresponding Mozley C800 concentrate (red circles) samples.

fluorocarbonates and monazite show a broad, irregular distribution (Figs. 7b and 8b).

3.2. Geochemistry

Pathfinder elements compatible with carbonatite indicator minerals (Table 1) were detected geochemically in all samples downstream from the Aley (Table 6) and Lonnie (Table 7) carbonatites. Concentrations of Nb in raw samples from the Aley drainage range from 3000 to 10,000 ppm with an average of 5900 ppm (Table 6). Niobium concentrations in corresponding Mozley concentrates are substantially higher, ranging from 11,900–25,900 ppm and averaging 17,600 ppm. Similarly, concentrations of Ta, Zr, LREE, U, Th, and P_2O_5 are higher in Mozley heavy mineral concentrates as compared to raw stream sediments. Relative to Aley, unprocessed samples from Lonnie have very low pathfinder elements concentrations (Table 7). Niobium ranges from 39 to 70 ppm and averages 53 ppm. Mozley C800 processing substantially increased the concentrations of all pathfinder elements with the exception of Ba. As noted previously, the Wicheeda samples were too small to be analyzed geochemically.

4. Discussion

This QEMSCAN® orientation survey focuses on samples from the Aley carbonatite drainage area for three reasons: 1) Aley has the largest number of stream sediment samples; 2) Aley is the most important carbonatite-related deposit in the Canadian Cordillera; and 3) pre-concentration of stream sediment samples from Aley is not required. Concentrations of pathfinder elements and indicator minerals are much lower in the Lonnie and Wicheeda areas (pre-concentration is required). Following pre-concentrations, the same QEMSCAN® methodology described for Aley can be applied to samples from Lonnie and Wicheeda.

4.1. Aley indicator mineralogy and geochemistry

4.1.1. Comparison of QEMSCAN® and geochemical analysis

The chemical compositions of samples derived from QEMSCAN® data (Table 5) and traditional laboratory analysis (Table 6) shows strong positive correlation (Fig. 10). Coefficients of determination between Nb ($R^2 = 0.90$; Fig. 10a), LREE ($R^2 = 0.91$; Fig. 10b), and Fe_2O_3 ($R^2 = 0.87$; Fig. 10c) determined by QEMSCAN® and laboratory chemical analysis indicates a predictable co-variation. The coefficient of determination (R^2) represents the goodness of fit to a trend line. An R^2 of 1.0 and trend line with slope of 1 and y-intercept of 0 would indicate perfect agreement between the two analytical methods; an R^2 of 0.90 indicates that 90% of the variation is explained by this relationship.

4.1.2. Comparison of indicator mineral abundance and pathfinder element concentration

There is a good fit between the concentration of carbonatite pathfinder elements (ppm or wt.%) determined for the raw 125–250 μm fraction and Mozley concentrate by geochemical analysis and the abundance of carbonatite indicator minerals determined by QEMSCAN® expressed as either mineral count or wt.%, however, the wt.% values correlate better than the particle counts. The highest coefficients of determination are obtained when comparing bulk sample chemistry and indicator mineral concentration in terms of wt.%. Niobium content is primarily related to pyrochlore ($R^2 = 0.72$; Fig. 11a) and columbite-(Fe) ($R^2 = 0.78$; Fig. 11b) abundance; fersmite is a minor contributor (Fig. 11c). Total niobate (sum of pyrochlore, columbite-[Fe], and fersmite) concentration ($R^2 = 0.90$; Fig. 11d) shows the best fit with Nb content of stream sediment samples. Surprisingly, R^2 for Nb content and fersmite abundance in Mozley concentrates is very high ($R^2 = 1.00$; Fig. 11c), even though fersmite is not abundant in the raw sample and its density (4.69–4.79; Table 1) is similar to that of pyrochlore (4.2–6.4) and less than that of columbite (5.3–7.3). This may be due in part to the tendency of the fersmite to occur in composite grains with the very dense columbite-(Fe), which also correlates well with fersmite in concentrates ($R^2 = 0.80$; Fig. 12). The LREE content of the concentrates is strongly related to monazite concentration ($R^2 = 0.91$; Fig. 11e) and less strongly to REE-fluorocarbonate concentration ($R^2 = 0.51$; Fig. 11f). Concentration of P_2O_5 in raw samples and corresponding concentrates is strongly related to apatite concentration ($R^2 = 0.98$; Fig. 11g) and weakly to monazite content ($R^2 = 0.25$; Fig. 11h). Thus, overall indicator mineral abundance measured by wt.% is broadly representative of bulk sample composition determined geochemically. The above relationships between traditional laboratory analysis and QEMSCAN® analysis indicate that mineralogical information from QEMSCAN® analysis on selected samples can provide the mineralogical context for interpreting relatively inexpensive and time efficient stream sediment geochemical surveys.

4.1.3. Mineral association in composite grains

A grain can consist of a single large mineral particle or as a composite grain. For example, the grain depicted in Fig. 3 is predominantly composed of a large apatite particle, with two smaller pyrochlore particle inclusions and numerous tiny mineral particle inclusions. Key mineral associations within composite grains and proportion of monomineralic grains are shown in Fig. 13 in relation to the proportion of monomineralic grains (wt.%). Pyrochlore (wt.%) is predominantly contained in composite grains composed of other minerals commonly associated with carbonatite magmatism and alteration (columbite-[Fe], apatite, fersmite, ±monazite; Fig. 13a, b) while apatite (wt.%) is observed mostly as monomineralic grains (Fig. 13j). Columbite-(Fe) (Fig. 13d), REE-fluorocarbonates (Fig. 13f), and monazite (Fig. 13h) fall in between these two extremes. Monazite occurring in association with pyrochlore, columbite-(Fe), fersmite, and apatite is inferred to be derived from carbonatite, whereas, monazite found in association with micas (chlorite, biotite, and muscovite), quartz, and other complex composite mineral grains ("Others" in Fig. 13) is probably sourced from clastic metasediments. Monomineralic monazite grains are assumed to be derived from carbonatite although their provenance is uncertain.

4.2. Lonnie indicator mineral abundance

The geochemical analyses for the three Lonnie stream sediment samples show consistently low concentrations of carbonatite pathfinder elements (Table 7). QEMSCAN® detected columbite-(Fe) in each sample (Tables 3 and 4). Pyrochlore was detected in only one of three raw samples (LO-13-02). All minerals except fersmite and barite were detected at wt.% levels in the Mozley concentrates (Table 3). This demonstrates that when indicator mineral concentrations in stream sediments are low, minimal processing enables QEMSCAN® analysis to detect and characterize carbonatite indicators.

4.3. Wicheeda indicator mineral abundance

All of the usual carbonatite indicator minerals were detected by QEMSCAN® in the three raw samples from Wicheeda (Tables 3 and 4) with the exception that no barite particles were found in one sample. Pyrochlore, columbite-(Fe), fersmite, monazite, REE-fluorocarbonates, zircon, magnetite, hematite, apatite, and barite are successfully concentrated by Mozley C800 processing.

4.4. Comparison of QEMSCAN with other methods

The QEMSCAN® methodology described in this study is able to quickly identify carbonatite indicator minerals in unprocessed stream sediments in high concentrations (e.g. Aley). In lower concentrations (e.g. Lonnie and Wicheeda) minimal processing allows QEMSCAN® to identify carbonatite indicator minerals. In both cases, QEMSCAN® can detect minerals at very small particle sizes, in low concentrations, and readily identify minerals that cannot be detected by traditional visual identification and hand-picking. This allows for smaller grain size fractions which contain higher abundances of indicator minerals to be studied.

The QEMSCAN® and minimal processing techniques as described in this study have comparable cost and much improved time efficiency compared to traditional visual identification and hand-picking of indicator minerals involving concentration by heavy liquid medium and isodynamic separation. The usefulness and potential of this technique is also highlighted by its wide availability in many industry laboratories and some academic institutions, and minimal operator training required. This study was able to detect many of the same indicator minerals as other studies (Lehtonen et al., 2011) which utilized automated

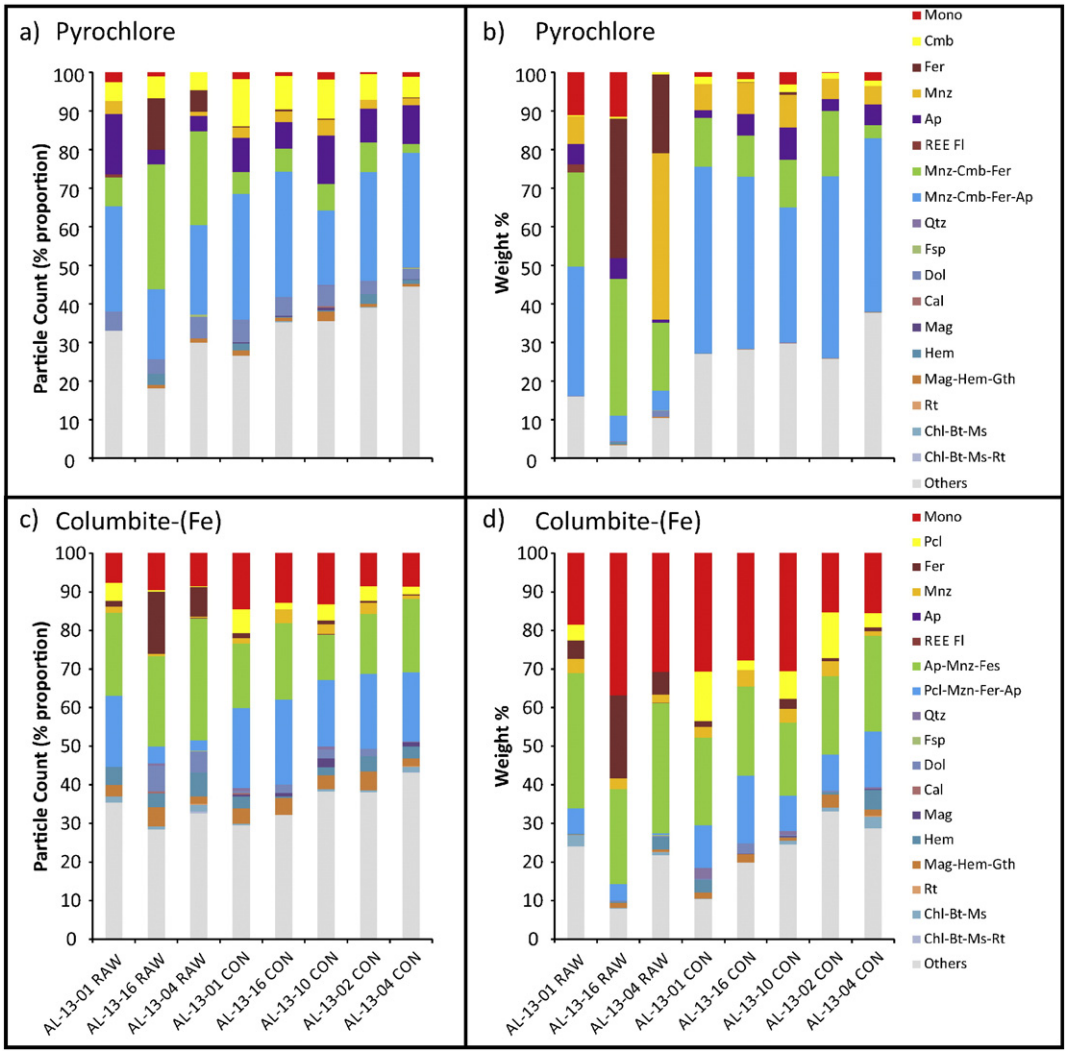

Fig. 13. Proportions of monomineralic (Mono) and composite grains with predominant mineral associations (in terms of mineral count and wt.%) for: a) and b) pyrochlore; c) and d) columbite-(Fe); e) and f) REE-fluorocarbonates; g) and h) monazite; i) and j) apatite. Results are for RAW samples and corresponding Mozley concentrates (CON). Sample distance increases from directly over the deposit (AL-13-04) to 11.5 km downstream (AL-13-01). 'Others' refer to very complex composite grains, and those containing unidentified mineral phases. Abbreviations: pyrochlore (Pcl); columbite-(Fe) (Cmb); fersmite (Fer); REE-fluorocarbonates (REE-Fl); zircon (Zrc); apatite (Ap); magnetite (Mag); hematite (Hem); rutile (Rt); amphibole/pyroxene (Amp/Px); barite (Brt); quartz (Qtz); dolomite (Dol); calcite (Cal); feldspar (Fsp); hematite (Hem); goethite (Gth); chlorite (Chl); biotite (Bt); and muscovite (Ms).

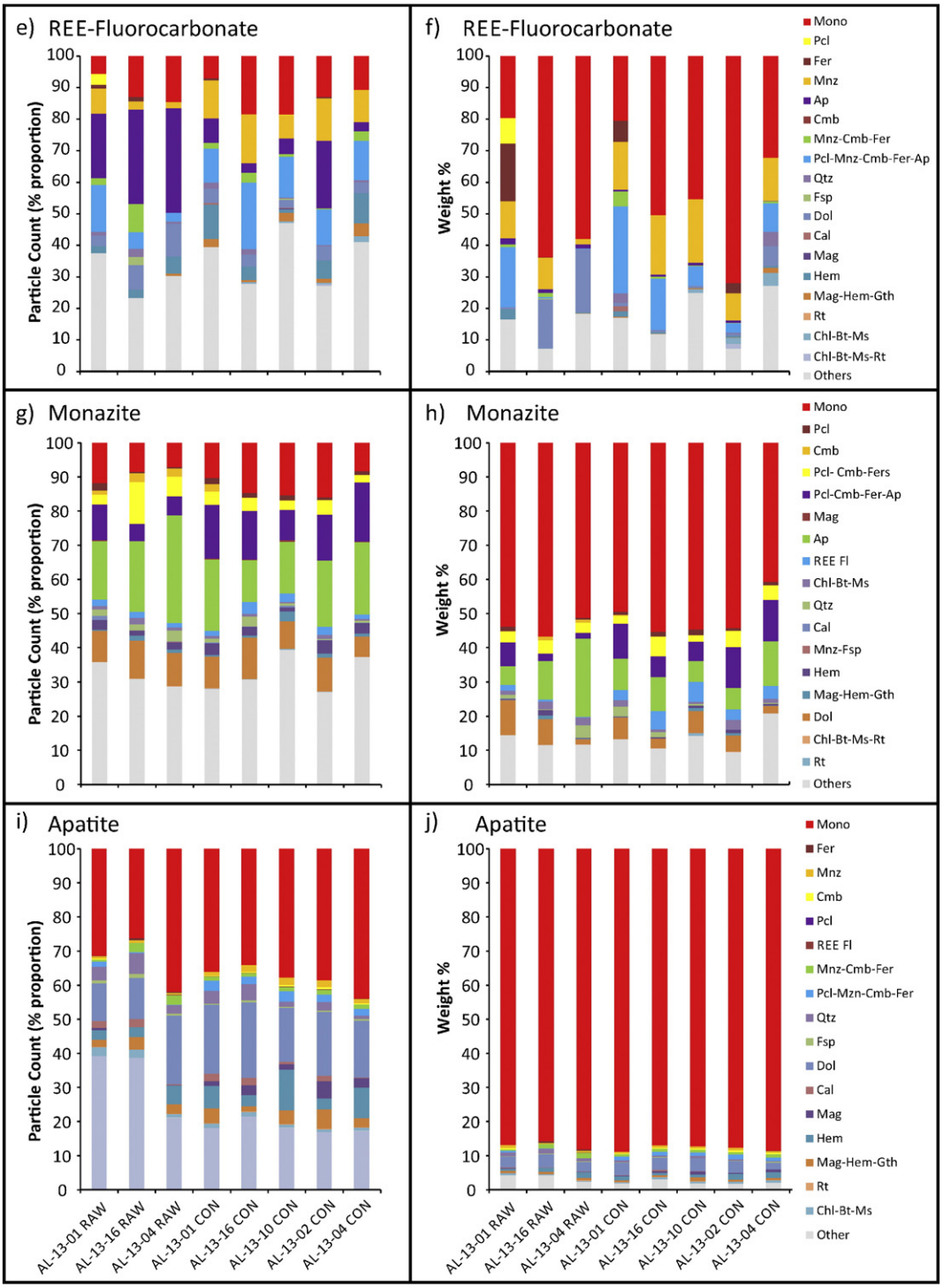

Fig. 13 (*continued*).

SEM techniques and more rigorous and time consuming processing methods (e.g. heavy liquids and isodynamic separation). This indicates that the simpler processing used in this study is a valuable time and cost saving step in indicator mineral studies.

With proper orientation surveys to help direct sample selection and identify the ideal size fraction for study, this method is applicable to stream and till sediments and has the potential to aid in the discovery of buried or poorly exposed carbonatite related Nb, Ta, and REE deposits.

5. Conclusions

With increased interest in carbonatite related specialty metal deposits, and the high potential for undiscovered deposits in Canada, new and optimized methods to explore for covered or poorly exposed carbonatites and related specialty metal deposits need to be developed. This study shows that QEMSCAN® can rapidly and effectively identify carbonatite indicator minerals in stream sediments with little to no additional processing by Mozley shaking table.

QEMSCAN® can detect indicator minerals in the dry sieved 125–250 μm fine sand size fraction of alluvial sediments downstream from the Aley, Lonnie and Wicheeda carbonatites without additional processing. If carbonatite pathfinder elements are in low concentration (e.g. samples from Lonnie), minimal preconcentration by Mozley C800 mineral separator can be used to increase the concentration of indicator minerals to detectable levels. This concentration technique can amplify geochemical indicator mineral anomalies that may be missed otherwise.

QEMSCAN® can detect and characterize particle sizes too small for traditional visual indicator mineral examination and hand-picking techniques and provides quantifiable proportions of monomineralic grains and mineral associations within composite grains. This is especially useful in REE exploration as associated mineralogy is often fine grained and very complex. QEMSCAN® can fully characterize a sample in 3.5 to 4.5 h using the 'Particle Mineral Analysis' routine, much faster than the 6 to 12 h required for traditional techniques to characterize a single sample with mineralogically complex grains. If the only mineral identification and their concentrations are needed, the Bulk Mineral Analysis routine can be used and analytical time is reduced to 30 min per sample. This compares favorably to the ~2 h required to visually identify and hand pick the indicator mineral grains. The QEMSCAN® method can also identify mineral particles much smaller than feasibly using optical methods. This allows for smaller grain size fractions which contain higher abundances of indicator minerals to be studied. As with this study, a careful and rigorous orientation survey is the best tool to optimize sample selection and processing techniques for a QEMSCAN® based indicator mineral study.

Acknowledgments

This project was supported by the Targeted Geoscience Initiative 4 (2010–2015), a Natural Resources Canada program. The Specialty Metal component of this program was carried out collaboratively between the Geological Survey of Canada and the British Columbia Geological Survey. Bureau Veritas Commodities Canada Ltd., Inspectorate Metallurgical Division and Acme Analytical Laboratories are thanked for access to laboratory equipment and the expert advice of their staff. We also thank Beth McClenaghan (Geological Survey of Canada), Stuart Averill (Overburden Drilling Management Limited), and David Lentz (Department of Geology, University of New Brunswick), for their thorough review, valuable suggestions, and constructive comments. Discussion and comments by Pearce Luck (British Columbia Geological Survey) greatly improved this manuscript. Helicopter and logistical support during sampling from Taseko Mines Limited and information provided by Jeremy Crozier (Hunter Dickinson Inc.) are greatly appreciated. The authors would also like to thanks Spectrum Mining Corporation for access to their deposit and core samples. Robert Lane (Plateau Minerals Corp.) and Chris Graf (Spectrum Mining Corporation) contributed to our understanding of the Wicheeda Lake carbonatite. Rara Terra Minerals Corp. allowed access to the Lonnie carbonatite showing. A scholarship from Geoscience BC to the first author is also appreciated.

References

Anthony, J.W., Biduaex, R.A., Bladh, K.W., Nichols, M.C., 2004. Handbook of Mineralogy. Mineralogical Society of America, Chantilly, U.S.A. (http://www.handbookofmineralogy.org/ Accessed December 29, 2014).

Atencio, D., Andrade, M.B., Christy, A.G., Gieré, R., Kartashov, P.M., 2010. The pyrochlore supergroup of minerals: nomenclature. Can. Mineral. 48, 673–698.

Averill, S.A., 2001. The application of heavy indicator mineralogy in mineral exploration with emphasis on base metal indicators in glaciated metamorphic and plutonic terrains. In: McClenaghan, M.B., Bobrowsky, P.T., Hall, G.E.M., Cook, S.J. (Eds.), Drift Exploration in Glaciated Terrain. Geological Society, London, Special Publications 185, pp. 69–81 (2001).

Averill, S.A., 2014. Indicator mineral fingerprints in surficial sediments near Cu–Au deposits of the porphyry–epithermal–volcanogenic suite. In: McClenaghan, M.B., Plouffe, A., Layton-Matthews, D. (Eds.), Application of Indicator Mineral Methods to Mineral Exploration. Geological Survey of Canada, Open File 7553, pp. 35–44 (2014).

Belousova, E.A., Griffin, W.L., O'Reilly, S.Y., Fisher, N.I., 2002a. Apatite as an indicator mineral for mineral exploration: trace-element compositions and their relationship to host rock type. J. Geochem. Explor. 76, 45–69.

Belousova, E.A., Griffin, W.L., O'Reilly, S.Y., Fisher, N.I., 2002b. Igneous zircon: trace element composition as an indicator of source rock type. Contrib. Mineral. Petrol. 143, 602–622.

Brod, J.A., 1999. Petrology and Geochemistry of the Tapira Alkaline Complex, Minas Gerais State, Brazil (Thesis) Durham University (http://etheses.dur.ac.uk/4971/).

Bühn, B., Wall, F., Le Bas, M.J., 2001. Rare-earth element systematics of carbonatitic fluorapatites, and their significance for carbonatite magma evolution. Contrib. Mineral. Petrol. 141, 572–591.

Černý, P., Ercit, T.S., 1985. Some recent advances in the mineralogy and geochemistry of Nb and Ta in rare-element granitic pegmatites. Bull. Mineral. 108, 499–532.

Černý, P., Ercit, T.S., Wise, M.A., 1992. The tantalite–tapiolite gap: natural assemblages versus experimental data. Can. Mineral. 30, 587–596.

Chakhmouradian, A.R., Reguir, E.P., Kressall, R.D., Crozier, J., Pisiak, L.K., Sidhu, R., Yang, P., 2015. Carbonatite-hosted niobium deposit at Aley, northern British Columbia (Canada): mineralogy, geochemistry and petrogenesis. Ore Geol. Rev. 64, 642–666.

Chisholm, E.O., 1960. Lonnie Columbian deposit. British Columbia Ministry of Energy and Mines Property File (<http://propertyfile.gov.bc.ca/showDocument.aspx?&docid=138373> accessed November 2014).

Graf, C., Lane, B., Morrison, M., 2009. The Wicheeda carbonatite–syenite breccia intrusive complex hosted rare earth deposit. Conference Abstract, 5th Annual Minerals South Conference and Trade Show, Cranbrook, Canada (<http://www.slideshare.net/RareMetalBelt/abstract-on-the-wicheeda-rare-earth-property#> Accessed December 13, 2013).

Hankinson, J.D., 1958. The Lonnie Group Columbium Deposit, Unpublished B.Sc. thesis, University of British Columbia, 32 p.

Jones, S., Merriam, K., Yelland, G., Rotzinger, R., Simpson, R.G., 2014. Technical Report on Mineral Reserves at the Aley Project, British Columbia, Canada. Taseko Mines Limited (291 p. <www.sedar.com> accessed February 3, 2015).

Kressall, R., McLeish, D.F., Crozier, J., 2010. The Aley carbonatite complex — part II petrogenesis of a cordilleran niobium deposit. In: Simandl, G.J., Lefebure, D.V. (Eds.), International Workshop on the Geology of Rare Metals, November 9–10, 2010, Victoria, Canada. Extended abstracts volume. British Columbia Ministry of Energy and Mines, British Columbia Geological Survey, Open File 2010-10, pp. 25–26.

Lane, B., 2009. Diamond drilling report on the Wicheeda property, Cariboo mining division. British Columbia Ministry of Energy, Mines, and Petroleum Resources, Assessment Report, p. 30873 (196 pp.).

Layton-Matthews, D., Hamilton, C., McClenaghan, M.B., 2014. Mineral chemistry: modern techniques and applications to exploration. In: McClenaghan, M.B., Plouffe, A., Layton-Matthews, D. (Eds.), Application of Indicator Mineral Methods to Mineral Exploration. Geological Survey of Canada, Open File 7553, pp. 9–18 (2014).

Lehtonen, M., Laukkanen, J., Sarala, P., 2011. Exploring RE and REE mineralization using indicator minerals. In: McClenaghan, B., Peuraniemi, V., Lehtonen, M. (Eds.), Indicator Mineral Methods in Mineral Exploration, Workshop 3, 25th International Applied Geochemistry Symposium, pp. 13–18.

Linnen, R.L., Trueman, D.L., Burt, R., 2014. Tantalum and niobium. In: Gunn, G. (Ed.), Critical Metals Handbook, first ed. John Wiley and Sons, Ltd., West Sussex, pp. 361–384.

Luck, P., Simandl, G.J., 2014. Portable X-ray fluorescence in stream sediment chemistry and indicator mineral surveys, Lonnie Carbonatite Complex, British Columbia. Geological Fieldwork 2013, British Columbia Ministry of Energy and Mines, British Columbia Geological Survey, Paper 2014-1, pp. 169–182.

Mackay, D.A.R., Simandl, G.J., 2014a. Geology, market and supply chain of niobium and tantalum—a review. Mineral. Deposita 49, 1025–1047.

Mackay, D.A.R., Simandl, G.J., 2014b. Portable X-ray fluorescence to optimize stream sediment chemistry and indicator mineral surveys, case 1: carbonatite-hosted Nb deposits, Aley carbonatite, British Columbia, Canada. Geological Fieldwork 2013a, British Columbia Ministry of Energy and Mines, British Columbia Geological Survey, Paper 2014-1, pp. 183–194.

Mackay, D.A.R., Simandl, G.J., 2014c. Portable X-ray fluorescence to optimize stream sediment chemistry and indicator mineral surveys, case 2: carbonatite-hosted REE deposits, Wicheeda Lake, British Columbia, Canada. Geological Fieldwork 2013b, British Columbia Ministry of Energy and Mines, British Columbia Geological Survey, Paper 2014-1, pp. 195–206.

Mackay, D.A.R., Simandl, G.J., 2015. Pyrochlore and columbite–tantalite as indicator minerals for specialty metal deposits. Geochem.: Explor., Environ., Anal. http://dx.doi.org/10.1144/geochem2014-289.

Mackay, D.A.R., Simandl, G.J., Grcic, B., Li, C., Luck, P., Redfearn, M., Gravel, J., 2015a. Evaluation of Mozley C800 laboratory mineral separator for heavy mineral concentration of stream sediments in exploration for carbonatite-related specialty metal deposits: case study at the Aley carbonatite, northeastern British Columbia (NTS 094B). Geoscience BC Summary of Activities 2014, Geoscience BC, Report 2015-1, pp. 111–122.

Mackay, D.A.R., Simandl, G.J., Luck, P., Grcic, B., Li, C., Redfearn, M., Gravel, J., 2015b. Concentration of carbonatite indicator minerals using a Wilfley gravity shaking table: a case history from the Aley carbonatite, British Columbia, Canada. Geological Fieldwork 2014, British Columbia Ministry of Energy and Mines, British Columbia Geological Survey, Paper 2015-1, pp. 189–195.

Mäder, U.K., 1986. The Aley Carbonatite Complex (Thesis) University of British Columbia (176 pp.).

Makin, S.A., Simandl, G.J., Marshall, D., 2014. Fluorite and its potential as an indicator mineral for carbonatite related rare earth element deposits. Geological Fieldwork 2013, British Columbia Ministry of Energy and Mines, British Columbia Geological Survey Paper 2014-1, pp. 207–212.

Mao, M., Rukhlov, A.S., Rowins, S.M., Spence, J., Coogan, L.A., 2015a. Detrital apatite trace-elements compositions: a robust new tool for mineral exploration. British

Columbia Ministry of Energy and Mines, British Columbia Geological Survey GeoFile 2015-09.

Mao, M., Simandl, G.J., Spence, J., Marshall, D., 2015b. Fluorite trace-elements chemistry and its potential as an indicator mineral: evaluation of LA-ICP-MS method. In: Simandl, G.J., Neetz, M. (Eds.), Symposium on Strategic and Critical Metals Proceedings, November 13–14, 2015, Victoria, British Columbia. British Columbia Ministry of Energy and Mines, British Columbia Geological Survey Paper 2015-3, pp. 251–264.

McClenaghan, M.B., 2011. Overview of common processing methods for recovery of indicator minerals from sediments and bedrock in mineral exploration. Geochem.: Explor., Environ., Anal. 11, 265–278.

McClenaghan, M.B., 2014. Overview of indicator mineral recovery methods for sediments and bedrock: 2013 update. In: McClenaghan, M.B., Plouffe, A., Layton-Matthews, D. (Eds.), Application of Indicator Mineral Methods to Mineral Exploration. Geological Survey of Canada, Open File 7553, pp. 1–7 (2014).

McCurdy, M.W., Prior, G.J., Friske, P.W.B., McNeil, R.J., Day, S.J.A., Nicholl, T.J., 2006. Geochemical, mineralogical and kimberlites indicator mineral electron microprobe data from silts, heavy mineral concentrates and water from a national geochemical reconnaissance stream sediment and water survey in northern and southwestern Buffalo Head Hills. Northern Alberta (Parts of 84B, 84C, 84F, and 84G): Alberta Energy and Utilities Board, Alberta Geological Survey, Special Report 76 and Geological Survey of Canada Open File 5057 (11 pp.).

McCurdy, M.W., Kjarsgaard, I.M., Day, S.J.A., McNeil, R.J., Friske, P.W.B., Plouffe, A., 2009. Indicator mineral content and geochemisty of stream sediments and waters from northeast British Columbia (NTS 94A, 94B, 94G, 94H, 94I, 94K, 94N, 94O, 94P). British Columbia Ministry of Energy and Mines, Geological Survey of British Columbia, Report 2009–2 and Geological Survey of Canada, Open File 6311 (19 pp.).

McLeish, D.F., 2013. Structure, Stratigraphy, and U–Pb Zircon–Titanite Geochronology of the Aley Carbonatite Complex, Northeast British Columbia: Evidence for Antler-Aged Orogenesis in the Foreland Belt of the Canadian Cordillera. Unpublished Master of Science thesis, University of Victoria, 131 p.

Pell, J., 1994. Carbonatites, nepheline syenites, kimberlites and related rocks in British Columbia. British Columbia Ministry of Energy, Mines and Petroleum Resources, British Columbia Geological Survey, Bulletin 88 (136 pp.).

Rowe, R.B., 1958. Niobium (columbium) deposits of Canada. Geological Survey of Canada, Economic Geology Series 18 (103 pp.).

Simandl, G.J., Reid, H.M., Ferri, F., 2013. Geological setting of the Lonnie niobium deposit, British Columbia, Canada. In: Geological Fieldwork 2012, British Columbia Ministry of Energy, Mines and Natural Gas, British Columbia Geological Survey, Paper 2013-1, pp. 127–138.

Simandl, G.J., Stone, R.S., Paradis, S., Fajber, R., Reid, H.M., Grattan, K., 2014. An assessment of a handheld X-ray fluorescence instrument for use in exploration and development with an emphasis on REEs and related specialty metals. Miner. Deposita 49, 999–1012.

Trofanenko, J., 2014. The Nature and Origin of REE Mineralization in the Wicheeda Carbonatite, British Columbia, Canada (Thesis) McGill University (173pp.).

Trofanenko, J., Williams- Jones, A.E., Simandl, G.J., 2014. The nature and origin of the carbonatite-hosted Wicheeda rare earth element deposit, British Columbia. Geological Fieldwork 2013, British Columbia Ministry of Energy and Mines, British Columbia Geological Survey Paper 2014-1, pp. 213–225.

Vartiainen, H., 1976. Solki: carbonatite prospecting by the heavy minerals in stream sediments. J. Geochem. Explor. 5, 335–337.